JOURNAL OF CATALYSIS 97, 137–149 (1986)

A Study of the Interactions of NO with Rh/TiO_2 and TiO_2-Promoted Rh/SiO_2

NUTAN K. PANDE AND ALEXIS T. BELL

Department of Chemical Engineering, University of California, Berkeley, California 94720

Received March 22, 1985; revised August 20, 1985

The interactions of NO with Rh/TiO_2 and TiO_2-promoted Rh/SiO_2 were studied by temperature-programmed desorption spectroscopy. The room-temperature chemisorption of NO was observed to decrease with increasing catalyst reduction temperature in a manner similar to that found for H_2 and CO. However, the adsorption capacity for NO was always substantially greater than that for H_2 or CO. The suppression of NO, CO, and H_2 chemisorption with increasing catalyst reduction temperature is attributed to the blockage of Rh adsorption sites by TiO_x moieties transferred from the support. The higher adsorption capacity for NO relative to H_2 and CO is ascribed to NO adsorption at anionic defects on portions of TiO_2 adjacent to Rh particles. NO desorption is accompanied by decomposition to form N_2O and N_2, the extent of decomposition increasing with decreasing Rh dispersion. While N_2O appears to be formed on the exposed surfaces of Rh particles, N_2 formation occurs on both Rh particles and the surface of the support.

INTRODUCTION

The activity of Group VIII metals for the synthesis of hydrocarbons from CO and H_2 has been shown to be significantly higher when these metals are supported on titania, rather than on silica or alumina (*1–8*). A similar enhancement in activity has also been reported recently for NO reduction with either H_2 or CO (*9*). In both cases, the increased activity of the titania-supported metal has been ascribed to the occurrence of metal–support interactions. While the exact nature of these interactions is not yet fully understood, there is an increasing body of evidence indicating that the changes in catalytic properties of small metal particles are due to a decoration of their surface by TiO_x moieties transferred from the TiO_2 support (*10–19*). These species physically block adsorption sites and may alter the adsorptive properties of the uncovered metal sites.

A large number of studies have been reported concerning the adsorption of H_2 and CO on titania-supported Group VIII metals (*20–23*), but relatively little is known about the interactions of NO with such catalysts. Recently, Fang and White (*24*) examined NO chemisorption on Pt/TiO_2 using infrared spectroscopy and volumetric chemisorption. They observed that NO chemisorption is suppressed following high-temperature reduction of the catalyst. This phenomenon was attributed to a transfer of electronic charge from the support to the Pt. In the present study, temperature-programmed desorption spectroscopy has been used to investigate the interactions of NO with Rh/TiO_2 and TiO_2-promoted Rh/SiO_2. These catalysts are of considerable interest since they exhibit very high activity for NO reduction (*9, 25*). The results of this study show that while the chemisorption of NO decreases with catalyst reduction temperature in a manner similar to that for H_2 and CO chemisorption, the amount of NO adsorbed is always greater than that of H_2 or CO. This and other features of NO adsorption and desorption are attributed to the interactions of NO with Rh, TiO_x moieties covering the Rh particles, and the TiO_2 support itself.

EXPERIMENTAL

Catalyst Preparation

The supported catalysts were prepared

0021-9517/86 $3.00

using $RhCl_3 \cdot 3H_2O$ (Aldrich Chemicals) as the metal precursor. The support materials used were Cab-O-Sil HS-5 Silica (BET surface area, 300 m^2/g) and Degussa P25 titania (BET surface area, 50 m^2/g). Samples of approximately 4 wt% Rh were prepared by incipient wetness impregnation of the support with a solution of $RhCl_3$ dissolved in deionized water. In addition, a sample of 0.5% Rh/TiO_2 was prepared by ion exchange using the method of Resasco and Haller (*26*). Following introduction of $RhCl_3$, each sample was dried overnight in a vacuum oven at 338 K, and calcined in a 21% O_2/He mixture at 773 K for 1 h.

A TiO_2-promoted Rh/SiO_2 sample was prepared in the following manner. A 4 wt% Rh/SiO_2 catalyst, prepared by impregnation of SiO_2 with a solution of $RhCl_3$, was dried but not calcined. This material was then impregnated with $Ti(OCH_3)_4$ (Alfa Chemicals) dissolved in 1 *N* HCl, by dropwise addition to the point of incipient wetness. The amount of $Ti(OCH_3)_4$ added corresponded to a Ti weight loading of 5%. A sample of TiO_2-promoted Rh black was prepared in a similar manner. The amount of $Ti(OCH_3)_4$ added to the Rh black (Aldrich Chemicals, 99.99% Rh), corresponded to a Ti weight loading of 1%. Both samples were dried overnight in a vacuum oven at 338 K, and then calcined in a 21% O_2/He mixture for 1 h. The TiO_2-promoted Rh black sample was calcined at 573 K and the TiO_2-promoted Rh/SiO_2 sample was calcined at 773 K.

Table 1 lists the Rh content and dispersion of Rh for all of the samples. The Rh weight loading of each sample was determined by X-ray fluorescence. The Rh dispersion was measured by volumetric chemisorption of H_2 at room temperature on samples which were reduced overnight at 573 K.

TABLE 1

Metal Content and Dispersion of Supported-Rh Catalysts

Catalyst	% Rh	Dispersion
Rh/SiO_2	4.60	0.55
Rh/TiO_2	4.33	0.26
Rh/TiO_2	0.51	0.55
TiO_2-Promoted Rh/SiO_2	4.70	0.25

Temperature-Programmed Desorption, Reduction, and Oxidation

The interaction of nitric oxide with the Rh catalysts was studied by temperature-programmed desorption. The apparatus used for these experiments has been described previously (*27*). A 30-mg sample of the catalyst was placed in a quartz microreactor and reduced in H_2 for at least 2 h at a temperature in the range of 523–773 K. The catalyst was then evacuated and ramped under vacuum to 823 K, to remove any adsorbed hydrogen. The sample was subsequently cooled under vacuum to room temperature. The microreactor was repressurized with helium, and NO was pulsed to the reactor to achieve saturation coverage. The catalyst was then ramped to 823 K at a linear heating rate of 1 K/s in a helium stream flowing at 50 cm^3/min. This procedure was repeated for successively higher reduction temperatures, and from the measured amount of NO, N_2O, and N_2 desorbed, the initial coverage of the adsorbate was determined as a function of catalyst reduction temperature. The above procedure was followed on all of the samples with the exception of the Rh black powder and the TiO_2-promoted Rh black powder. Due to concern that the unsupported metal powders would sinter if evacuated to 823 K, the powders were evacuated at the sample reduction temperature and then cooled under vacuum to room temperature.

Temperature-programmed reduction was performed on the samples after calcination in a 21% O_2/He mixture at 623 K for 2 h. The sample was cooled to room temperature and a mixture of 1000 ppm H_2/He was flowed through the reactor at 50 cm^3/min. The sample was then ramped to 823 K at a linear heating rate of 1 K/s and the rate of H_2 consumption was monitored.

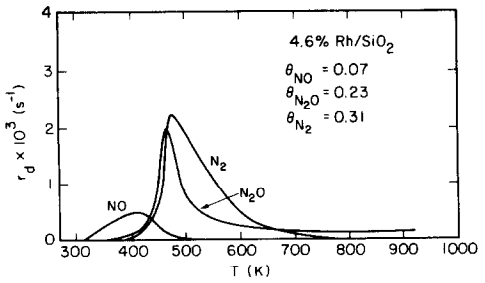

FIG. 1. NO TPD spectrum for 4.6% Rh/SiO_2 after reduction at 573 K.

Temperature-programmed oxidation was performed on the samples after reduction in H_2 at 573 K overnight. The sample was cooled to room temperature and a mixture of 1000 ppm O_2/He was flowed through the reactor at 50 cm^3/min. The sample was then ramped to 823 K at a linear heating rate of 1 K/s and the rate of O_2 consumption was monitored.

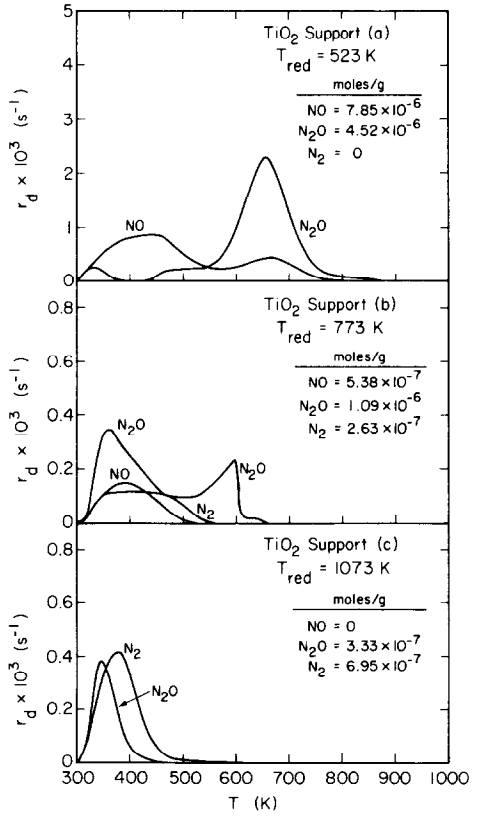

FIG. 2. NO TPD spectra for TiO_2 support reduced at 523 K (a), 773 K (b), and 1073 K (c).

RESULTS

4.6% Rh/SiO_2 Catalyst

The NO desorption spectrum for the Rh/SiO_2 catalyst reduced at 573 K is shown in Fig. 1. The appearance of N_2O and N_2, in addition to NO, is indicative of NO decomposition. Single peaks are observed for NO and N_2O, centered at 425 and 475 K, respectively. The spectrum for N_2 is comprised of two components, a narrow peak at 475 K and a broad peak centered at 550 K. The initial coverage of NO was determined from the total quantity of nitrogen containing products desorbed and corresponds to $\theta_{NO}^{\circ} = 0.61$.

TiO_2 Support

TPD spectra taken after reduction of the TiO_2 support at 523, 773, and 1073 K are shown in Fig. 2. The spectrum obtained following reduction at 523 K shows (Fig. 2a) peaks for both NO and N_2O. The presence of N_2O is indicative of NO disproportionation. Two broad peaks are observed for NO, centered at 425 and 675 K. N_2O formation reaches a maximum rate of 660 K, but a small N_2O peak centered at 333 K is also apparent. When the support reduction temperature is increased from 523 to 773 K

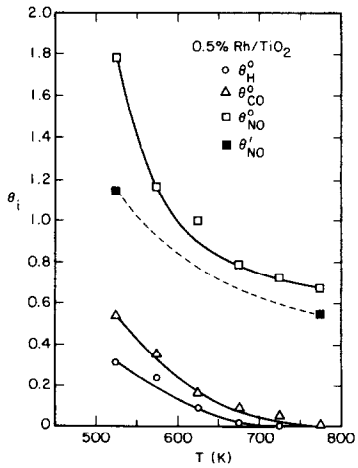

FIG. 3. Effect of catalyst reduction temperature on the adsorption capacity of H_2, CO and NO for 0.5% Rh/TiO_2.

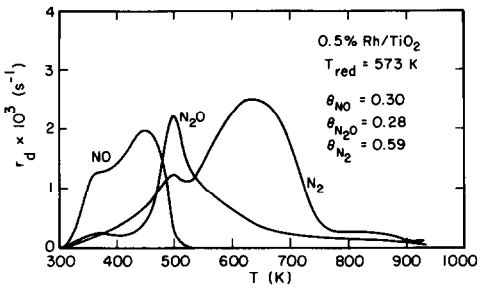

FIG. 4. NO TPD spectrum for 0.5% Rh/TiO_2 after reduction at 573 K.

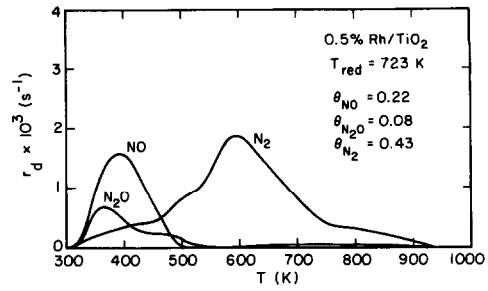

FIG. 6. NO TPD spectrum for 0.5% Rh/TiO_2 after reduction at 723 K.

(Fig. 2b), the amount of NO adsorbed decreases from 1.73×10^{-5} to 3.24×10^{-6} mol/g. The TPD spectrum is also altered by reduction at 773 K. As seen in Fig. 2c, nearly equivalent peaks for NO, N_2O, and N_2 are now observed near 353 K. A smaller N_2O peak still appears though at 575 K. Raising the reduction temperature to 1073 K reduces the uptake of NO to 2.05×10^{-6} mol/g. In this case, the TPD spectrum shows no evidence for desorbed NO, and N_2O and N_2 are the only nitrogen-containing products observed. The temperatures at maximum rate of N_2O and N_2 formation are 353 and 385 K, respectively.

0.5% Rh/TiO_2 Catalyst

The total uptake of NO on 0.5% Rh/TiO_2 was determined by integration of the spectra for nitrogen-containing products produced during temperature-programmed desorption. The results are shown in Fig. 3, as a function of catalyst reduction temperature. The dashed curve represents a correction of the total NO uptake to account for NO adsorbed on the support itself. Curves for the uptakes of H_2 and CO, reported previously (*11*), are also shown for comparison. It is immediately evident that while the uptakes of NO, CO, and H_2 all decrease in a similar manner with increasing catalyst reduction temperature, the uptake of NO is substantially greater than that of CO and H_2 in all cases. This distinctive feature of NO chemisorption is evident most clearly for reduction at 773 K, at which point H_2 and CO chemisorption are completely suppressed but 0.55 of a Rh monolayer of NO is still chemisorbed.

TPD spectra taken after reduction of the 0.5% Rh/TiO_2 sample at 573, 673, 723, and 773 K are shown in Figs. 4 through 7. Peaks for NO, N_2O, and N_2 are observed in each of these figures. For reduction at 573 K, two NO peaks are seen, centered at 353 and 458 K. The N_2O spectrum shows a small peak at 353 and a large peak at 493 K, which has a tail extending to higher temperatures. The

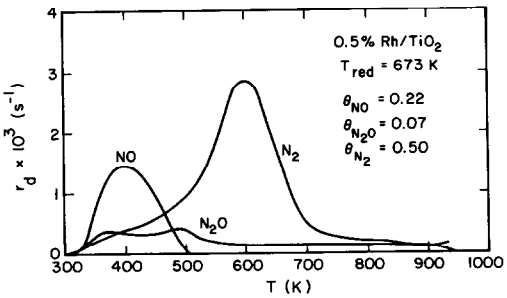

FIG. 5. NO TPD spectrum for 0.5% Rh/TiO_2 after reduction at 673 K.

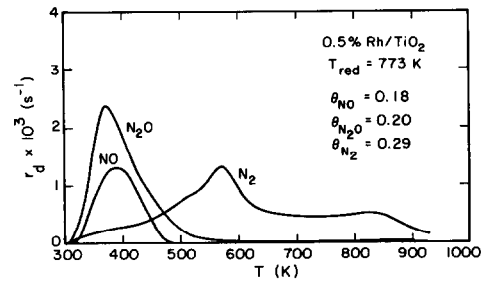

FIG. 7. NO TPD spectrum for 0.5% Rh/TiO_2 after reduction at 773 K.

N_2 spectrum exhibits two small peaks at 353 and 823 K, a medium-sized peak at 493 K, and a large, broad peak at 633 K. As the catalyst reduction temperature is increased, the two NO peaks coalesce, the N_2O peak at 493 K diminishes while that at 353 K grows, and the center of mass of the N_2 spectrum shifts to higher temperatures.

The recovery of NO adsorption capacity was also examined. After reduction of the catalyst at 773 K, it was stored in a dessicator at room temperature for over a month. The sample was then reduced at 523 K. The TPD spectrum for adsorbed NO is shown in Fig. 8. The positions, shapes, and relative intensities of all of the features seen in Fig. 8 bear much more resemblance to those shown in Fig. 4, than to those in Fig. 7. It is also evident from the tabulated data that the NO adsorption capacity of the high-temperature reduced sample was partially restored by long-term exposure to air.

4.3% Rh/TiO_2 Catalyst

The desorption of NO from the 4.3% Rh/TiO_2 catalyst was studied as a function of catalyst pretreatment. This sample was not reduced at successively higher reduction temperatures, but instead was cycled from high-temperature to low-temperature reduction with intermediate calcination at 773 K. The purpose of this procedure was to determine if calcination of the catalyst would cause it to regain its initial capacity for NO adsorption. Table 2 summarizes the results as a function of catalyst pretreatment. It is evident that after high-temperature reduction, pretreatment of the catalyst by high-temperature calcination and subsequent reduction at low temperature only partially restores the NO chemisorption capacity. The NO desorption spectra for the 4.3% Rh/TiO_2 catalyst taken after reduction at 573 and 673 K are shown in Figs. 9 and 10, respectively. The N_2 peak tails out to higher temperatures and the N_2O peak desorption is shifted to lower temperatures when the reduction temperature is raised from 573 to 673 K. This is the same trend that was observed for the 0.5% Rh/TiO_2 catalyst.

TABLE 2

Effect of Pretreatment on NO Adsorption Capacity for 4.3% Rh/TiO_2

Pretreatment	θ°_{NO}
Reduced at 573 K	1.15
Reduced at 673 K	0.45
Calcined at 773 K (1 h) and reduced at 623 K	0.48
Calcined at 773 K (1 h) and reduced at 573 K	0.74

TiO_2-Promoted 4.7% Rh/SiO_2 Catalyst

The NO adsorption capacity for the TiO_2-promoted 4.7% Rh/SiO_2 catalyst is shown in Fig. 11 as a function of catalyst reduction temperature. The uptakes of H_2 and CO reported previously (*11*) are also shown. The change in adsorptive capacity with reduction temperature for this catalyst is very

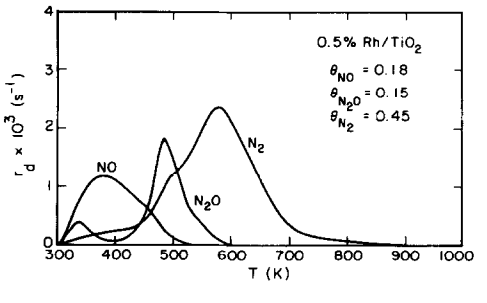

FIG. 8. NO TPD spectrum for 0.5% Rh/TiO_2 initially reduced at 773 K, exposed to air at room temperature for one month, and then reduced at 523 K.

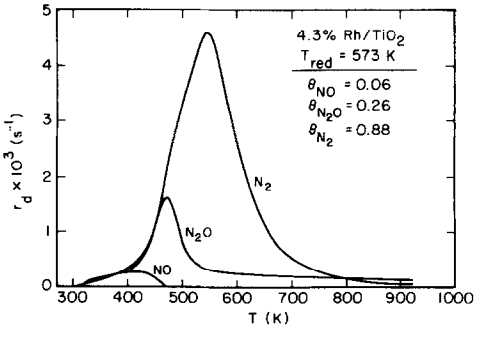

FIG. 9. NO TPD spectrum for 4.3% Rh/TiO_2 after reduction at 573 K.

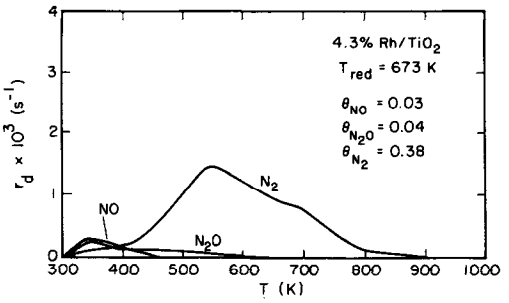

FIG. 10. NO TPD spectrum for 4.3% Rh/TiO_2 after reduction at 673 K.

similar to that seen in Fig. 3 for 0.5% Rh/TiO_2. Here again, the capacity for NO adsorption decreases with increasing reduction temperature, but is always larger than the adsorption capacity for CO or H_2.

Figure 12 shows the NO TPD spectrum for the TiO_2-promoted 4.7% Rh/SiO_2 catalyst after reduction at 523 K. Most of the adsorbed NO desorbs as N_2 in two overlapping peaks centered at 498 and 548 K. Small peaks for NO and N_2O are also seen at 423 and 483 K, respectively. As the catalyst reduction temperature increases, the peaks for NO and N_2O disappear completely, and the N_2 spectrum extends out to higher and higher temperatures. These trends are clearly seen in Fig. 13.

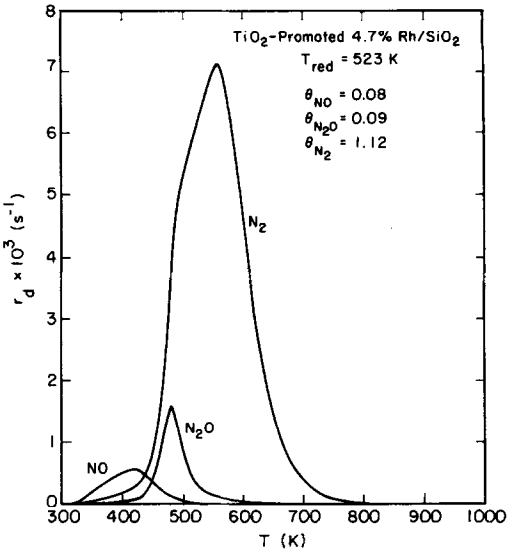

FIG. 12. NO TPD spectrum for TiO_2-promoted 4.7% Rh/SiO_2 after reduction at 523 K.

Rh Black and TiO_2-Promoted Rh Black

The interactions of NO with Rh black and TiO_2-promoted Rh black were also investigated. TPD spectra taken following adsorption of NO are shown in Fig. 14. In contrast to the supported-Rh catalysts, N_2 is the only product observed. For Rh black, the N_2 peak is at 453 K but is shifted to 753 K for TiO_2-promoted Rh black. The amount

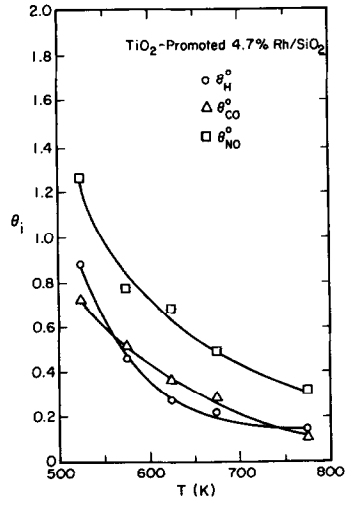

FIG. 11. Effect of catalyst reduction temperature on the adsorption capacity of H_2, CO, and NO for TiO_2-promoted 4.7% Rh/SiO_2.

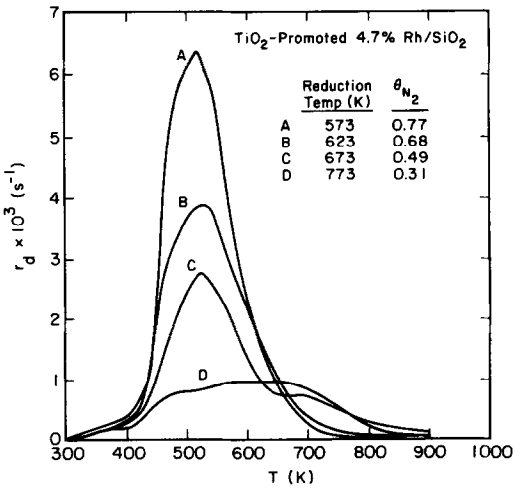

FIG. 13. NO TPD spectra for TiO_2-promoted 4.7% Rh/SiO_2 after reduction at 573 K (A), 623 K (B), 673 K (C), and 773 K (D).

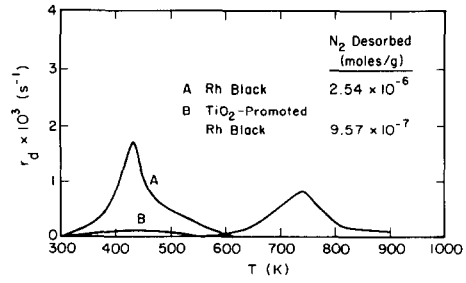

FIG. 14. NO TPD spectra for Rh black (A) and TiO_2-promoted Rh black (B) after reduction at 523 K.

of NO adsorbed on Rh black is 2.54×10^{-6} and 9.57×10^{-7} mol/g for TiO_2-promoted Rh black. Since both samples were reduced at the same temperature, 523 K, the observed differences in N_2 peak position are directly due to the influence of TiO_2 on the Rh-black particles.

Temperature-Programmed Reduction and Oxidation

Temperature-programmed reduction of the TiO_2 support showed no evidence for H_2 uptake over the entire temperature range. Temperature-programmed oxidation was performed on the TiO_2 support after reduction in H_2 overnight at 523 K. Oxygen consumption was noticeable starting at 473 K and continued up to 823 K. Since it was suspected that this oxygen uptake might be due to oxygen deficiencies in the TiO_2 lattice, temperature-programmed oxidation was performed on an untreated TiO_2 sample. Oxidation was observed starting at 473 K and continued up to 823 K; the support consumed 1.5×10^{-5} mol O_2/g TiO_2 (1.2×10^{-3} mol O_2/mol TiO_2). It should be noted that O_2 consumption was measured only up to 823 K. O_2 was still being consumed at this temperature. These results indicate that the untreated TiO_2 support is not fully oxidized.

Figure 15 shows the results for temperature-programmed reduction of the 4.6% Rh/SiO_2 sample and the 0.5% Rh/TiO_2 sample. A single sharp H_2 consumption peak is seen at 373 K for the Rh/SiO_2 sample. Prior to temperature-programmed reduction of the Rh/SiO_2 catalyst, the sample was calcined in a 21% O_2/He mixture for 2 h at 623 K. Under these conditions, all of the rhodium should be converted to rhodium oxide. If it is assumed that because of the rapid heating rate (1 K/s) during temperature-programmed reduction only the surface of the oxide particles are reduced and that an H atom remains adsorbed on each surface Rh atom, the following stoichiometry will be obeyed:

$$Rh_2O_3 + 4H_2 \rightarrow 2Rh{-}H + 3H_2O.$$

Thus the H_2 consumption should be $2H_2$ per Rh surface site. The sample used for the temperature-programmed reduction experiment contains 7.28×10^{-6} mol of surface Rh sites. So theoretically, the H_2 consumption should be 1.46×10^{-5} mol H_2. The experimentally measured H_2 consumption was 1.48×10^{-5} mol H_2. The excellent agreement between these latter two figures indicates that the sharp H_2 consumption peak corresponds to reduction of surface rhodium oxide to rhodium metal. A sharp H_2 consumption peak is also observed for the Rh/TiO_2 sample, this time at 393 K.

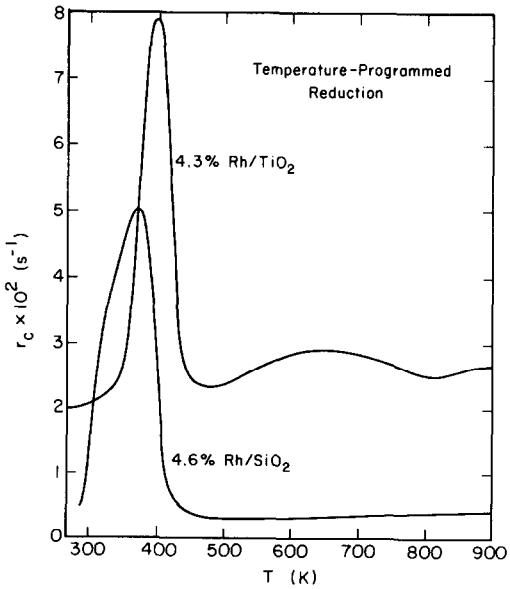

FIG. 15. H_2 consumption during TPR of calcined 4.6% Rh/SiO_2 and 0.5% Rh/TiO_2.

However, in addition, there is a broad H_2 consumption peak starting at 473 K and centered at about 673 K. Assuming that the first low-temperature peak corresponds to reduction of surface rhodium oxide, the theoretical H_2 consumption should be 8.34 $\times 10^{-6}$ mol H_2. The measured H_2 consumption is 7.37 $\times 10^{-6}$ mol H_2, in reasonable agreement with that predicted. The broad, high-temperature H_2 consumption peak, not observed for the Rh/SiO_2 catalyst, is assumed to be due to reduction of the TiO_2 support. This peak corresponds to a H_2 consumption of 0.84 equivalents of a Rh monolayer. It should be noted that there was no H_2 consumption for temperature-programmed reduction of the TiO_2 support by itself, so it appears that the presence of the Rh metal is essential for reduction of the TiO_2 support. In this connection, it is important to recognize that the transmission electron microscopy studies, selected-area electron diffraction and X-ray diffraction have confirmed that the support of a Rh/TiO_2 catalyst does not undergo bulk reduction for temperatures up to 1073 K (*11*). Thus, it appears that the role of the Rh metal particles is to produce a source of H_a which can then reduce TiO_2 in the vicinity of the metal particles, thereby forming TiO_x species.

Temperature-programmed oxidation of the Rh/SiO_2 sample showed no oxygen consumption over the entire temperature range, but it was noticed that the oxygen signal dropped considerably when a 1000 ppm O_2/He mixture was flowed over the reduced catalyst at room temperature. It is assumed that the reduced metal takes up a monolayer of oxygen at room temperature and that there is no further oxidation. In contrast, the temperature-programmed oxidation of the 0.5% Rh/TiO_2 sample showed O_2 consumption at room temperature as well as during the ramp in 21% O_2/He. Figure 16 shows the resulting O_2 consumption spectrum. There is a broad peak centered at 623 K and O_2 is still being consumed even at 823 K. The measured O_2 consumption was 1.56 $\times 10^{-5}$ mol O_2/g catalyst. This corresponds closely to the O_2 uptake of the TiO_2 support in the absence of Rh.

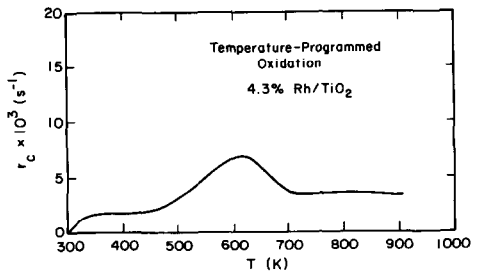

FIG. 16. O_2 consumption during TPO of reduced 0.5% Rh/TiO_2.

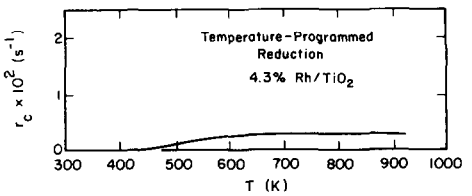

FIG. 17. H_2 consumption during TPR for 4.3% Rh/TiO_2 following NO TPD.

Temperature-programmed reduction experiments were also used to verify that oxygen released during the temperature-programmed desorption of nitric oxide from a Rh/TiO_2 catalyst is taken up by partially reduced titania. Figure 17 shows the results for temperature-programmed reduction of the 4.3% Rh/TiO_2 catalyst following a NO TPD experiment. A large H_2 consumption peak is observed at room temperature, which is attributed to the reduction of O atoms on the Rh metal at room temperature. In addition, as shown in Fig. 17, a broad H_2 consumption peak is evident starting at 473 K. The area under this peak corresponds to 0.75 equivalents of a Rh monolayer. The results of temperature-programmed reduction experiments on prereduced Rh/TiO_2 have shown that there is no further reduction, thus it is concluded that the peak observed in Fig. 17 is due to the reduction of titania which was oxidized during the NO TPD process.

DISCUSSION

Unsupported Rh

The interactions of NO with unsupported Rh have been investigated previously by a number of authors (*28–35*). The results obtained with polycrystalline samples and with various single crystal surfaces are qualitatively similar. For low coverages ($\theta_{NO} \lesssim 0.5$), NO adsorbs dissociatively and the only product observed in the TPD spectra is N_2. At higher NO coverages, a small amount of NO is observed to desorb prior to the formation of N_2. The N_2 signal is composed of two overlapping peaks. It has been proposed that the low-temperature peak is due to the process $N_a + NO_a \rightarrow N_2 + O_a + S$, whereas the high-temperature peak is due to the process $2N_a \rightarrow N_2 + 2S$. With the exception of Castner and Somorjai (*29*), none of the authors working with unsupported Rh have reported the formation of N_2O. Castner and Somorjai (*29*) observed the appearance of a small amount of N_2O in studies carried out with Rh (331) and Rh(S) − [6(111) × (100)] surfaces. It was proposed that N_2O might form via reactions such as $2NO_a \rightarrow N_2O + O_a + S$ and $N_a + NO_a \rightarrow N_2O + 2S$.

The shape of the N_2 spectrum for Rh black presented in Fig. 14 is quite similar to that reported by Campbell and White (*34*) for polycrystalline Rh foil. The absence of NO or N_2O during temperature-programmed desorption suggests that the dissociation of NO on Rh black is very efficient.

Rh/SiO_2

The TPD spectrum for 4.6% Rh/SiO_2 presented in Fig. 1 is similar to that reported by Chin and Bell (*36*) for a 5% Rh/SiO_2 catalyst. The principal difference is that Chin and Bell (*36*) observed a higher proportion of the adsorbed NO (~85%) decomposed to N_2 upon elevation of the catalyst temperature. This difference can be ascribed to the much lower Rh dispersion (16.4%) of the catalyst used by Chin and Bell compared to that used in the present studies (55%). As will be discussed below for Rh/TiO_2, the fraction of adsorbed NO decomposing to N_2 increases with decreasing dispersion. Further supporting this conclusion is the observation that on Rh black, which has a dispersion of 0.35%, all of the adsorbed NO decomposes to N_2.

In their study, Chin and Bell (*36*) demonstrated that the TPD spectrum for NO desorption and decomposition can be interpreted using the following reaction sequence:

(1) $NO_a \rightleftarrows NO + S$
(2) $NO_a + S \rightarrow N_a + O_a$
(3) $NO_a + N_a \rightarrow N_2O + 2S$
(4) $NO_a + N_a \rightarrow N_2 + O_a + S$
(5) $2Na \rightarrow N_2 + 2S$

Rate parameters for each elementary steps were determined by fitting simulated TPD spectra to those observed experimentally.

Structure and Composition of Rh/TiO_2 and TiO_2-Promoted Rh/SiO_2

The physical and chemical characteristics of titania-supported Group VIII metals have been studied extensively with the aim of explaining what causes the suppression of H_2 and CO chemisorption following high-temperature reduction of such catalysts (*10–19, 22, 37–40*). The most convincing interpretation is that derived from AES observations which suggests that the loss of chemisorption capacity is due to the decoration of the supported-metal crystallites by TiO_x moieties. These species modify the metal surface not only by physical blockage but also through a change of the electronic properties of metal atoms near the TiO_x moieties (*10–19*).

Recent electron microscopy studies of Rh/TiO_2 and TiO_2-promoted Rh/SiO_2, reported by Singh *et al.* (*11*), lend further support to the decoration model. Regions of amorphous titania were observed at the periphery of Rh particles supported on TiO_2, following high-temperature reduction. Likewise, micrographs of TiO_2-promoted Rh/SiO_2 showed evidence of crystal-

line TiO_2 platelets after such catalysts were reduced at 773 K. Platelet formation appeared to be nucleated by the Rh particles and did not occur in the absence of the metal. Defocussing experiments confirmed that the TiO_2 platelets were situated on top of the Rh particles. Based on these observations it was concluded that the suppression of H_2 and CO chemisorption for Rh/TiO_2 and TiO_2-promoted Rh/SiO_2 is due to the deposition of an amorphous layer of TiO_x over the particles, which upon heating in H_2 is converted to crystalline TiO_2.

While studies by Baker and coworkers (*10, 37–40*) have indicated that TiO_2 undergoes partial reduction to Ti_4O_7 in the presence of supported Group VIII metals, selected-area electron diffraction and X-ray diffraction of the catalysts used in this study showed no evidence for such transformations (*11*). In fact, the only changes seen were a gradual conversion of anatase to rutile when the reduction temperature was 1073 K. The TPR spectra presented in Fig. 15 show, however, that a portion of the support does lose oxygen upon reduction above 500 K. Since no loss of oxygen was observed from TiO_2, it is concluded that Rh is required to promote the reduction of TiO_2, in agreement with previous studies (*37, 41–44*). The portion of the TiO_2 undergoing reduction cannot be defined unambiguously. We propose, however, that it is the TiO_x moieties covering the Rh particles or portions of TiO_2 adjacent to the Rh particles. Elevation of the reduction temperature, thus, appears to have two effects—one is to increase the coverage of Rh particles by TiO_x and the second is to increase the extent of reduction of the TiO_x species in the proximity of the Rh particles.

NO Adsorption on TiO_2

The TPD spectra in Fig. 2 clearly demonstrate that NO will adsorb to a small degree on TiO_2 in the absence of Rh. The influence of TiO_2 reduction temperature on the distribution of products formed during desorption provides indirect evidence of a change in the composition of the support surface, even though no bulk reduction occurs (*11*).

When the TiO_2 is reduced at 773 and 1073 K, the desorption of N_2O and N_2 occurs at much lower temperatures than when the support is reduced at 523 K. It is also evident that the fraction of adsorbed NO appearing as N_2O and N_2 increases with increasing reduction temperature. These observations suggest that a small amount of the TiO_2 surface does undergo reduction in H_2 even in the absence of Rh, and that dissociative adsorption of NO can occur at these partially reduced centers.

NO Adsorption on Rh/TiO_2 and TiO_2-Promoted Rh/SiO_2

The data presented in Figs. 3 and 11 demonstrate that the room-temperature chemisorption of NO on 0.5% Rh/TiO_2 and TiO_2-promoted 4.7% Rh/SiO_2 decreases as the catalyst reduction temperature increases. However, the amount of NO adsorbed always exceeds the amount of H_2 or CO chemisorbed by a fixed quantity. This pattern can be explained by assuming that NO adsorbs both on the exposed portions of Rh crystallites (i.e., those not covered by TiO_x) and on partially reduced titania present in the vicinity of the Rh particles. Since the amount of NO absorbed in excess of CO or H_2 is greater for the 0.5% Rh/TiO_2 catalyst than the TiO_2-promoted 4.7% Rh/SiO_2 catalyst, the concentration of reduced titania must be greater for the former catalyst. It should also be noted that NO adsorption on the TiO_x moieties covering the Rh particles does not appear to occur, for if it did, the extent of decrease in NO adsorption with reduction temperature would not be as large as that seen in Figs. 3 and 11.

The interactions of NO with silica- and titania-supported Rh are quite different. For example, while the 4.6% Rh/SiO_2 and the 0.5% Rh/TiO_2 samples have the same dispersion, the fraction of nitrogen containing species desorbed as NO, following reduction at 573 K, is much larger for the titania-supported catalyst. The position and

shapes of the N_2 spectra are also different for the two catalysts. For 0.5% Rh/TiO_2, and N_2 spectrum exhibits large peaks at 493 and 633 K and smaller peaks at 353 and 823 K. The N_2 spectrum for 4.6% Rh/SiO_2 has a large peak at 475 K which overlaps a broad peak centered at about 550 K. The absence of N_2 peaks above 573 in the spectra for Rh black and Rh/SiO_2 reported here, strongly suggests that the N_2 peaks appearing at 633 and 823 K in the spectrum of 0.5% Rh/TiO_2 are due to the desorption of nitrogen atoms attached to Ti ions rather than Rh atoms. Moreover, it is conceivable that the 633 K peak may be associated with Ti ions in contact with Rh surface atoms and the 823 K peak, with Ti ions not in contact with Rh surface atoms. The attribution of these two high-temperature peaks to nitrogen atom adsorption on Ti ions is supported by the shift in the N_2 peak for Rh black from 453 to 753 K when the sample is promoted with TiO_2 (see Fig. 14). By contrast to what is observed for N_2, the spectra for N_2O produced over 4.6% Rh/SiO_2 and 0.5% Rh/TiO_2 are remarkably similar in position and shape. This suggests that most of the N_2O is produced on the Rh particles for both catalysts.

Figures 4–7 demonstrate that the spectra of nitrogen-containing products observed for 0.5% Rh/TiO_2 change substantially as the catalyst reduction temperature increases. For a reduction temperature of 573 K, the NO spectrum is made up of two overlapping peaks centered at 353 and 458 K. With increasing reduction temperature, the intensity of the second peak diminishes somewhat, while that of the first remains nearly constant. Inspection of Figs. 1 and 2 suggests that the peak at 458 K in Fig. 4 is attributable, at least in part, to NO desorbing from Rh particles, whereas the peak at 353 K is due primarily to NO desorption from the TiO_2 support. The decrease in intensity of the peak at 458 K with increasing reduction temperature can then be ascribed to a progressive increase in the fraction of Rh particles covered by TiO_x moieties.

The N_2O spectrum seen in Fig. 4 has a small peak at about 353 K and a large, well-defined peak at 493 K. As the reduction temperature increases, the high-temperature feature rapidly disappears, whereas the low-temperature feature grows. This is particularly evident for reduction temperatures above 700 K. The coincidence of the N_2O and NO peaks near 353–373 K, following high-temperature reduction of 0.5% Rh/TiO_2 is similar to that observed in the spectra of TiO_2 (Fig. 2) suggesting that the N_2O peak at 353 K is due to N_2O formation on the partially reduced support. As noted above, the similarity of the positions and shapes of the N_2O peak seen at 475–493 K in the spectra of 4.6% Rh/SiO_2 and 0.5% Rh/TiO_2 indicates that this feature arises from the process $N_a + NO_a \rightarrow N_2O + 2S$ occurring on the surface of Rh particles. The decrease in intensity of the N_2O peak with increasing reduction temperature observed in the spectra for 0.5% Rh/TiO_2 is ascribed to the progressive coverage of the Rh particles by TiO_x.

Two principal changes occur in the N_2 spectrum with increasing reduction temperature. The peak at 573 K decreases, while that at 823 K increases in intensity. As discussed earlier, the first of these peaks is attributed to N_2 formation involving species adsorbed on the Rh particles, whereas the second peak is attributed to N_2 formation involving N atoms attached to Ti cations. The absence of the 823 K peak from the spectrum observed for reduced TiO_2 (Fig. 2) suggests that the Ti cations may be those associated with TiO_x moieties covering the Rh particles. Such an interpretation would be consistent with the change in relative intensity of the peaks at 573 and 823 K with increasing reduction temperature.

The spectra of nitrogen-containing products observed for 4.3% Rh/TiO_2 are qualitatively similar to those observed for 0.5% Rh/TiO_2. The primary difference is that a smaller fraction of the initially adsorbed NO is released as NO. This would suggest that more of the NO dissociates upon ad-

sorption on 4.3% Rh/TiO_2 than on 0.5% Rh/TiO_2. The most plausible interpretation is that the extent of NO dissociation increases with decreasing Rh dispersion. As shown in Table 1, the dispersion of 0.5% Rh/TiO_2 is 55%, while that for 4.3% Rh/TiO_2 is 26%.

The spectra obtained for TiO_2-promoted 4.7% Rh/SiO_2 very closely resemble the spectra for 4.3% Rh/TiO_2 but differ significantly from those for 4.6% Rh/SiO_2. This gives strong evidence of the influence of TiO_2 moieties interacting with Rh on the adsorption/desorption behavior of NO. The low proportion of nitrogen-containing products appearing as NO or N_2O again suggests that a substantial portion of the NO adsorbed initially is dissociated. This interpretation is supported by the prominence of the N_2 peak at 548 K relative to that at 498 K. As discussed earlier, the first of these peaks is due to $2N_a \rightarrow N_2 + 2S$, whereas the latter is due to $N_a + NO_a \rightarrow N_2 + O_a + S$. Once again, the change in the shape of the N_2 spectrum with increasing catalyst reduction temperature can be attributed to a progressive decoration of the Rh particles by TiO_x.

The suppression of NO chemisorption following high-temperature reduction of Rh/TiO_2 catalysts can be partially restored by oxidation of the catalyst (see Table 2). Moreover, comparison of Figs. 4 and 8 demonstrates that room-temperature oxidation of Rh/TiO_2 after reduction at 773 K results in a restoration of the TPD spectrum observed upon reduction at 573 K. The mechanism by which the adsorption capacity is partially restored via oxidation has not yet been established. One possibility is that upon raising the oxygen content of the TiO_x moieties covering the Rh particles, these structures no longer wet the Rh particles as effectively. Contraction of the TiO_x moieties or their migration back to the support would result in a large fraction of the metal surface being exposed.

CONCLUSIONS

The results of the present study demonstrate that NO chemisorption is suppressed with increasing catalyst reduction temperature for Rh/TiO_2 and TiO_2-promoted Rh/SiO_2. While this trend is similar to that observed for H_2 and CO chemisorption, the amount of NO adsorbed is significantly larger than the amount of H_2 or CO adsorbed. The suppression of NO chemisorption with increasing reduction temperature is believed to result from physical blockage of rhodium surface sites by TiO_x moieties transferred from the support. Such structures also block the chemisorption of CO and H_2. The higher adsorption capacity for NO relative to CO and H_2 is ascribed to NO adsorption on partially reduced sites present on portions of titania immediately adjacent to rhodium crystallites. These adsorption sites are formed by spillover of atomic hydrogen from rhodium crystallites onto the support and subsequent reduction of a portion of the support surface.

Desorption of NO from Rh/TiO_2 and TiO_2-promoted Rh/SiO_2 is accompanied by decomposition to form N_2O and N_2. The extent of decomposition increases with decreasing Rh dispersion. While N_2O appears to be formed primarily on the exposed surfaces of rhodium particles, N_2 formation takes place on both the rhodium particles and the support. The latter process is believed to involve the recombination of nitrogen atoms bound to titanium ions.

ACKNOWLEDGMENT

This work was supported by the National Science Foundation through Grant CEP82-16537.

REFERENCES

1. Solymosi, F., Tombacz, I., and Kocsis, M., *J. Catal.* **75,** 78 (1982).
2. Katzer, J. R., Sleight, A. W., Gajardo, P., Michel, J. B., Gleason, E. F., and McMillan, S., *Faraday Discuss. Chem. Soc.* **72,** 121 (1982).
3. Bracey, J. D., and Burch, R., *J. Catal.* **86,** 384 (1984).
4. Ozdogan, S. Z., Gochis, P. D., and Falconer, J. L., *J. Catal.* **83,** 257 (1983).

5. Vannice, M. A., and Garten, R. L., *J. Catal.* **66,** 242 (1980).
6. Ryndin, Y. A., Hicks, R. F., and Bell, A. T., *J. Catal.* **70,** 287 (1981).
7. Burch, R., and Flambard, A. R., *J. Catal.* **78,** 389 (1982).
8. Vannice, M. A., and Garten, R. L., *J. Catal.* **56,** 236 (1979).
9. Pande, N. K., and Bell, A. T., *Appl. Catal.*, in press.
10. Simoens, A. J., Baker, R. T. K., Dwyer, D. J., Lund, C. F. K., and Madon, R. J., *J. Catal.* **86,** 359 (1984).
11. Singh, A. K., Pande, N. K., and Bell, A. T., *J. Catal.* **94,** 422 (1985).
12. Santos, J., Phillips, J., and Dumesic, J. A., *J. Catal.* **81,** 147 (1983).
13. Resasco, D. E. and Haller, G. L., *J. Catal.* **82,** 279 (1983).
14. Jiang, X., Hayden, T. F., and Dumesic, J. A., *J. Catal.* **83,** 168 (1983).
15. Cairns, J. A., Baglin, E. E., Clark, G. J., and Zeigler, J. F., *J. Catal.* **83,** 301 (1983).
16. Sadeghi, H. R., and Henrich, V. E., *J. Catal.* **87,** 279 (1984).
17. Takatani, S., and Chung, Y. W., *J. Catal.* **90,** 75 (1984).
18. Chung, Y. W., Xiong, G., and Kao, C., *J. Catal.* **85,** 237 (1984).
19. Belton, D. N., Sun. Y.-H., and White, J. M., *J. Amer. Chem. Soc.* **106,** 3059 (1984).
20. Tauster, S. J., Fung, S. C., and Garten, R. L., *J. Amer. Chem. Soc.* **100,** 170 (1978).
21. Tauster, S. J., Fung, S. C., and Garten, R. L., *J. Catal.* **55,** 29 (1978).
22. Imelik, B., Naccache, C., Coudurier, G., Praliaud, H., Meriaudeau, P., Allezat, P., Martin, G. A., and Vedrine, J. C., Eds., *Stud. Surf. Sci. Catal.* **11** (1982).
23. Tauster, S. J., Fung, S. C., Baker, R. T. K., and Horsley, J. A., *Science (Washington, D.C.)* **211,** 1121 (1981).
24. Fang, S. M., and White, J. M., *J. Catal,* **83,** 1 (1983).
25. Rives-Arnau, V., and Munuera, G., *Appl. Surf. Sci.* **6,** 122 (1980).
26. Resasco, D. E., and Haller, G. L., *Stud. Surf. Sci. Catal.* **11,** 105 (1982).
27. Low, G., and Bell, A. T., *J. Catal.* **57,** 397 (1979).
28. Castner, D. G., Sexton, B. A., and Somorjai, G. A., *Surf. Sci.* **71,** 519 (1978).
29. Castner, D. G., and Somorjai, G. A., *Surf. Sci.* **83,** 60 (1979).
30. Baird, R. J., Ku, R. C., and Wynblatt, *Surf. Sci.* **97,** 346 (1980).
31. Ho, P., and White, J. M., *Surf. Sci.* **137,** 103 (1984).
32. Dubois, L. H., Hansma, P. K., and Somorjai, G. A., *J. Catal.* **65,** 318 (1980).
33. Miki, H., Kioka, T., and Kawasaki, K., *Surf. Sci.* **121,** 218 (1982).
34. Campbell, C. T., and White, J. M., *Appl. Surf. Sci.* **1,** 347 (1978).
35. Root, T. W., Schmidt, L. D., and Fischer, G. B., *Surf. Sci.* **134,** 30 (1983).
36. Chin, A. A., and Bell, A. T., *J. Phys. Chem.* **87,** 3700 (1983).
37. Baker, R. T. K., Prestridge, E. B., and Garten, R. L., *J. Catal.* **56,** 390 (1979).
38. Baker, R. T. K., Prestridge, E. B., and Garten, R. L., *J. Catal.* **59,** 293 (1979).
39. Baker, R. T. K., Prestridge, E. B., and Murrell, L. L., *J. Catal.* **79,** 348 (1983).
40. Baker, R. T. K., Prestridge, E. B., and McViker, G. M., *J. Catal.* **89,** 422 (1984).
41. Apple, T. M., Gajardo, P., and Dybowski, C., *J. Catal.* **68,** 103 (1981).
42. Apple, T. M., and Dybowski, C., *J. Catal.* **71,** 316 (1981).
43. Apple, T. M., and Dybowski, C., *Surf. Sci.* **121,** 243 (1982).
44. Vis, J. C., Van't Blik, F. J., Huizanga, T., Van Grondelle, J., and Prins, R., *J. Mol. Catal.* **25,** 367 (1984).